

# Application of Hematite Synthesized from Iron Rust Waste as a Pigment Dyes for Cotton Textile Printing

Asiyah Nurrahmajanti<sup>1\*</sup>, Octianne Djamaluddin\*, Wulan Safrihatini Atikah\*

\* Textile Chemistry Study Program, Politeknik STTT Bandung, Indonesia

## Article Info

### Article history:

Received May 7<sup>th</sup>, 2026

Accepted Jun 29<sup>th</sup>, 2026

Published Jul 1<sup>st</sup>, 2026

### Corresponding Author:

<sup>1</sup>Asiyah Nurrahmajanti  
Textile Chemistry Study  
Program  
Politeknik STTT Bandung

Email:

[asiyah.rahma@kemenperi.go.id/](mailto:asiyah.rahma@kemenperi.go.id)

[asiyah.janti@gmail.com](mailto:asiyah.janti@gmail.com)

## ABSTRACT

Iron rust is an abundant waste material with potential to be utilized as an iron oxide pigment. While previous studies have focused on its synthesis, its application in textile printing remains limited. This study evaluates the performance of hematite (Fe<sub>2</sub>O<sub>3</sub>) derived from iron rust waste as a pigment for cotton fabric printing. The pigment was incorporated into a conventional printing formulation and applied onto cotton fabric. Color strength (K/S), CIELAB properties, and fastness to washing and rubbing were evaluated with five replicates to ensure data reliability. The results show a slight increase in K/S from  $1.13 \pm 0.09$  to  $1.22 \pm 0.10$  with increasing synthesis concentration, although the difference remains moderate. The printed fabrics exhibited consistent reddish-yellow hues and low variability in colorimetric values, indicating good reproducibility. Washing fastness was acceptable (grade 3 for color change; 4–5 for staining), while rubbing fastness ranged from 2–4. These findings demonstrate that rust-derived hematite is applicable as a pigment in textile printing. However, performance is influenced by pigment–binder interaction, indicating the need for further optimization to improve color strength and durability.

**Keyword:** Iron rust, hematite, pigment dyes, textile printing

## 1. INTRODUCTION

Iron rust is a naturally occurring corrosion product that inevitably forms when iron or steel is exposed to oxygen and moisture. Although various preventive methods—such as galvanization, cathodic protection, and protective coatings—have been developed, environmental conditions remain unpredictable, allowing rust formation to persist (Bennett, 2019). Recent studies highlight that iron rust waste may hold added value as a raw material for synthesizing iron oxide-based functional materials.

Previous research demonstrates several innovative applications of rust-derived iron oxides. Li et al. (2025) employed rust as a co-catalyst in photocatalytic hydrogen production (Li et al., 2025). Cahyana et al. (2024) synthesized Fe<sub>3</sub>O<sub>4</sub> nanoparticles from rust waste for organic synthesis catalysis (Cahyana et al., 2024). Whereas Chavan et al. (2024) produced Fe<sub>2</sub>O<sub>3</sub> nanoparticles for applications in triboelectric generators, dye adsorption, and biomedical hyperthermia therapy (Chavan et al., 2024).

In recent years, increasing attention has been directed toward the development of sustainable materials derived from industrial and environmental waste. Iron rust, which is commonly generated from corrosion processes in infrastructure and manufacturing sectors, represents an abundant yet underutilized resource. Instead of being discarded, this waste can be

transformed into valuable iron oxide materials, contributing to waste minimization and resource efficiency. Such approaches are aligned with the principles of green chemistry and circular economy, which emphasize the conversion of low-value waste into functional products with minimal environmental impact (Chavan et al., 2024; Fiuza et al., 2018).

The extensive use of synthetic dyes in the textile industry has raised significant environmental concerns due to the generation of large volumes of colored wastewater containing toxic and non-biodegradable compounds. These effluents pose serious risks to aquatic ecosystems and human health, thereby necessitating the development of more sustainable coloration alternatives (Katheresan et al., 2018; Yaseen & Scholz, 2019).

Iron oxide pigments, particularly hematite ( $\alpha\text{-Fe}_2\text{O}_3$ ), have been widely used in ceramics, paints, polymers, and construction due to their stability, durability, and non-toxic nature (Cornell & Schwertmann, 2003; Fiuza et al., 2018; Pfaff, 2020). Hematite can be synthesized from machining waste and iron-rich residues (Fakhrudin, 2019; Habibah, 2019; Legodi & de Waal, 2007). Despite the extensive use of iron oxide pigments in coatings, ceramics, and construction materials, their application in the textile industry remains relatively limited. Textile coloration traditionally relies on synthetic dyes, which often involve complex chemical processes and may generate hazardous effluents. In contrast, pigment-based coloration offers a more environmentally friendly alternative, as it does not require chemical bonding with the fiber and typically involves fewer processing steps. However, the use of inorganic pigments such as hematite in textile printing is still underexplored, particularly in terms of performance optimization and compatibility with standard textile processing conditions (Choudhury, 2022; Yilidirim et al., 2020).

Although several studies have reported the synthesis of iron oxide pigments from various waste sources, limited research has focused on their direct application in textile printing systems. Previous works mainly emphasize synthesis methods and physicochemical characterization, while fewer studies evaluate their functional performance on textile substrates, particularly regarding color strength and fastness properties. Furthermore, the relationship between pigment characteristics—such as particle size and dispersion—and textile performance remains insufficiently explored (Fiuza et al., 2018; Legodi & de Waal, 2007).

This study addresses this gap by investigating the application of hematite synthesized from iron rust waste as a pigment for cotton textile printing. Unlike previous studies that primarily focus on material synthesis, this work emphasizes practical application and performance evaluation under standardized textile testing conditions. The results are expected to provide insight into the feasibility of utilizing rust-derived hematite as a sustainable and functional pigment alternative in textile coloration systems.

## 2. RESEARCH METHOD

### 2.1 Materials and Instruments

Iron rust waste was collected from corroded iron materials and used as the raw precursor for hematite synthesis. Hydrochloric acid (HCl 1 M and 4 M), sodium hydroxide (NaOH 4 M), and distilled water were used as chemical reagents. Cotton fabric (100%, Ready for Print, RFP) was used as the substrate. The printing paste consisted of binder (175 g/L), diammonium phosphate (DAP, 10 g/L), urea (100 g/L), and thickener adjusted to a total volume of 1 L. Instrumentation included a laboratory oven, furnace, magnetic stirrer, pH meter, analytical balance, and a 3NH Grating Benchtop Spectrophotometer for color measurement.

### 2.2 Synthesis of Hematite Pigment

The synthesis of hematite is based on (Nurrahmajanti & Lisdiana, 2025) without any modification through an acid leaching-precipitation-calcination method. Initially, iron rust waste was dissolved in hydrochloric acid solution with variation concentration 1 M and 4 M. Therefor for the clarity it will be mention as H1M and H4M. The dissolution taken under continuous stirring for

60 minutes at room temperature to extract iron ions. The resulting solution was filtered to remove insoluble residues. The filtrate was then subjected to precipitation by slowly adding sodium hydroxide solution 4 M until the pH reached approximately 8, resulting in the formation of a brown precipitate ( $\text{Fe}(\text{OH})_3$ ). The precipitate was aged for 1 hour, filtered, and washed repeatedly with distilled water until neutral pH was achieved. The obtained precipitate was dried in an oven at  $110^\circ\text{C}$  for 1 hour and subsequently calcined in a furnace at  $700^\circ\text{C}$  for 2 hours to produce hematite ( $\text{Fe}_2\text{O}_3$ ) pigment. The obtained pigment was ground into fine powder prior to use in printing applications.

### 2.3 Printing Procedure

Printing process in this research is using flat printing method as shown in Figure 1. Initially, the prepared printing paste was mixed with hematite pigment at a concentration of 20 g/L and homogenized thoroughly. After that, the cotton fabric was laid flat on the printing table without folds. The screen was positioned over the fabric, and the printing paste was poured onto the top of the screen. The screen is held in place to prevent it from shifting on the fabric. A rakel was used to evenly transfer the paste. After printing, the fabric was dried using a stenter at  $100^\circ\text{C}$  followed by heat-fixed at  $150^\circ\text{C}$  to ensure proper pigment fixation.

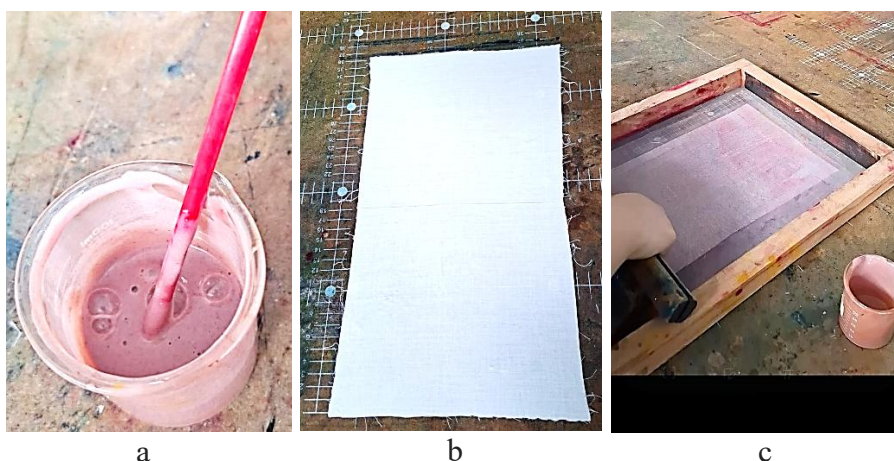


**Figure 1.** Printing processing. a) Printing paste, b) Cotton fabric RFP, and c) Flat printing using hematite pigment dyes

### 2.4 Testing and Analysis

#### a. Color Properties Measurement

Color measurements were performed according to CIELAB 1976 using a 3NH Grating Benchtop Spectrophotometer. The 3NH Grating Benchtop Spectrophotometer and its adapter were connected to a laptop. The spectrophotometer was powered on by pressing the power button, and the Texforma software was launched. Instrument calibration was performed using a standard calibration plate and a white reference plate. After calibration, measurements of K/S,  $L^*$ ,  $a^*$ , and  $b^*$  values were first conducted on the white fabric. Subsequently, the same parameters (K/S,  $L^*$ ,  $a^*$ ,  $b^*$ ,  $C^*$ , and  $h^\circ$  were recorded to determine hue and chromaticity) were measured on the test fabric samples. All measured values were displayed and recorded via the laptop interface. Measurements were conducted at 490 nm, calculated using the Kubelka–Munk equation. Five replications were performed for each variation and the results were expressed as mean  $\pm$  standard deviation.

#### b. Washing Fastness

Washing Fastness was evaluated according to SNI ISO 105-C06:2010. The test specimen is cut to a size of  $4 \times 10$  cm, and the lining fabric is cut according to the required dimensions. The test specimen and the multifiber (rayon, acetate, cotton, nylon, polyester, acrylic, wool) lining fabric are stitched together at the top edge. The washing solution is prepared by dissolving 4 g/L of ECE WOB

detergent soap in distilled water. The washing solution is poured into a stainless-steel container. The solution temperature is adjusted according to the specified standard (40°C), then the test specimen and 1 steel balls are placed inside, and the container is closed. The machine is operated at 40°C for 45 minutes. The test specimen is removed and rinsed twice with 100 mL of distilled water for 1 minute at 40°C. It is then rinsed again with 100 mL of distilled water for 1 minute and wrung out. The test specimen is dried by hanging at a temperature not exceeding 60°C. The color change of the test specimen is evaluated using the gray scale, and staining on the lining fabric is assessed using the staining scale.

### c. Rubbing Fastness

Rubbing fastness was tested according to SNI ISO 105-X12:2016 using a crockmeter. Details in follow:

- Dry rubbing

The test specimen is placed on the testing device with its long side aligned in the direction of the rubbing motion. The crockmeter finger is wrapped with dry white cotton fabric and placed on the specimen, then rubbed back and forth 10 times (equivalent to 20 rubs) by turning the crank 10 times at a speed of one rotation per second. The white cotton is then removed and evaluated for color staining.

- Wet rubbing

The white cotton cloth is moistened with distilled water, then pressed between filter papers so that the water content becomes  $65 \pm 5\%$  of the weight of the test specimen. The crockmeter finger is wrapped with the wet white cotton and placed on the test fabric, then rubbed back and forth 10 times (20 rubs) by turning the crank 10 times quickly to prevent evaporation. The white cloth is air-dried before evaluation. The white cotton is then removed and assessed for color staining.

## 3. RESULTS AND ANALYSIS

The hematite pigment used in this study was synthesized from iron rust waste using an acid leaching–precipitation–calcination method, as reported in our previous work (Nurrahmanti & Lisdiana, 2025). In that study, the synthesis parameters and chemical transformation of iron rust into  $\text{Fe}_2\text{O}_3$  were systematically investigated.

In the present study, the synthesized hematite is utilized without further modification to evaluate its applicability as a pigment in textile printing systems. Therefore, this work focuses primarily on assessing functional performance, including color strength, color properties, and fastness behavior on cotton fabric. Although detailed physicochemical characterization of the synthesized hematite has been reported previously, its performance in textile applications has not yet been explored. Thus, this study provides new insight into the practical utilization of rust-derived hematite as a sustainable pigment for textile printing. This application-oriented approach differentiates the present work from previous studies, which predominantly focused on synthesis and characterization rather than end-use performance in textile systems.

The results of this study demonstrate that hematite synthesized from iron rust waste can be used effectively as a pigment dyes for printing cotton fabric printing. The printed samples exhibited visually uniform coloration without noticeable defects such as patchiness or uneven pigment distribution, indicating that the pigment was adequately dispersed within the printing paste as shown in Figure 2. The fixation mechanism of hematite pigment on cotton fabric is primarily governed by the formation of a polymeric binder film rather than chemical bonding with the fiber. Since hematite ( $\text{Fe}_2\text{O}_3$ ) is an inorganic pigment lacking reactive functional groups, it cannot form covalent interactions with cellulose chains. Instead, adhesion occurs through physical entrapment within the binder matrix and weak intermolecular forces such as van der Waals interactions (Choudhury, 2022).

During the curing stage at elevated temperature (150°C), the binder undergoes film formation and crosslinking, resulting in a continuous polymer network that encapsulates pigment

particles and anchors them onto the fiber surface. This mechanism is consistent with the general principles of pigment printing, where durability depends strongly on binder film integrity and adhesion to the substrate (Choudhury, 2022; Yilidirim et al., 2020)

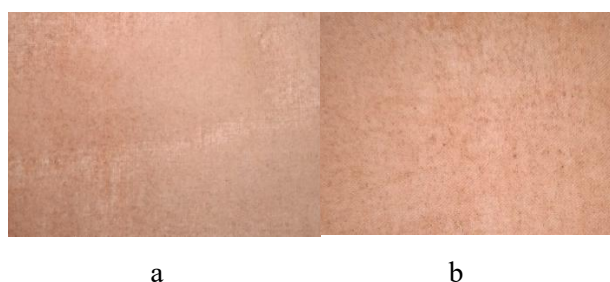


**Figure 2.** Results of printed cotton using hematite pigment dyes. a) H1M and b) H4M

In addition to the pigment itself, the composition of the printing paste plays a crucial role in determining the final performance. The presence of urea contributes to moisture retention during drying, facilitating better film formation. Diammonium phosphate (DAP) acts as a catalyst that promotes crosslinking reactions during curing, enhancing binder fixation. Meanwhile, the thickener controls paste viscosity, ensuring uniform application and preventing pigment migration. The synergy between these components significantly influences both color uniformity and fastness properties.

### 3.1 Color Strength (K/S Values)

The color strength result show an increased from 1.13 (H1M) to 1.22 (H4M) confirm that higher pigment concentration enhances surface coloration. According to the Kubelka–Munk theory, color strength (K/S) is determined by the relationship between the absorption (K) and scattering (S) coefficients of the colorant layer. An increase in pigment concentration may enhance light absorption, leading to higher color intensity when absorption dominates over scattering (Choudhury, 2014). The K/S results are summarized below in Table 1.

**Table 1.** Color Strength (K/S)



Variation	K/S Value	Average K/S	Standard Deviation
H1M	1.08	1.13	0.0942
	1.01		
	1.14		
	1.26		
	1.17		
H4M	1.15	1.22	0.1018
	1.31		
	1.35		
	1.12		
	1.18		

However, the relatively moderate K/S values observed in this study suggest that factors beyond concentration, may be attributed to particularly particle size and morphology, play an important role. Inorganic pigments such as hematite generally possess larger particle sizes, which increase light scattering and limit penetration into the fiber structure, thereby reducing color depth. Additionally, non-uniform particle distribution may affect optical properties and surface smoothness. In comparison with literature, inorganic pigments such as hematite typically exhibit lower K/S values than organic dyes due to higher light scattering and lower absorption efficiency

(Fiuza et al., 2018; Pfaff, 2020). In addition, the standar deviation showed <1 (0.09-0.10) means that the levelness of the printed fabric is good.

Furthermore, the CIELAB 1976 color properties ( $L^*$ ,  $a^*$ ,  $b^*$ ,  $C^*$ ,  $h^\circ$ ) demonstrate consistent color characteristics across all replicates as shown in **Table 2**. According to Cornell & Schwertmann (2003), hematite generally presents  $a^*$  (9 – 11) and  $b^*$  (7 – 9) values in the positive region, corresponding to red and yellow chromaticity which is consistent with their intrinsic electronic structure and light absorption behavior (Cornell & Schwertmann, 2003). The  $L^*$  values obtained in this study indicate that the printed fabrics exhibit relatively moderate brightness, suggesting that the pigment layer does not fully obscure the substrate. A slight decrease in  $L^*$  with increasing pigment concentration reflects darker coloration due to increased surface coverage. Meanwhile, the chroma ( $C^*$ ) values indicate moderate color saturation, which is typical for inorganic pigments such as hematite. The hue angle ( $h^\circ$ ) values ranging between  $35^\circ$ – $40^\circ$  confirm the dominance of reddish-yellow tones, characteristic of  $Fe_2O_3$  pigments which is likely influenced by crystal structure and particle size distribution (Khoiroh et al., 2013). These results demonstrate that pigment concentration influences not only color strength but also perceived brightness and saturation.

**Table 2.** Color Characteristics

Variation	Color Characteristic Values					Appearance
	$L^*$	$a^*$	$b^*$	$c^*$	$h$	
<b>H1M</b>	59.43	9.96	7.4	12.41	36.6	
	59.81	9.53	6.91	11.77	35.95	
	58.88	10.04	8.63	13.24	40.69	
	57.54	10.55	8.04	13.26	37.30	
	58.78	10.23	7.45	12.42	36.82	
<b>H4M</b>	58.78	10.23	8.23	13.13	38.80	
	56.48	9.69	7.04	11.97	36.01	
	57.07	11.33	9.40	14.72	39.67	
	58.58	9.6	6.97	11.86	35.96	
	58.51	10.15	8.13	13.01	38.68	

### 3.2 Rubbing Fastness

The rubbing fastness values for iron oxide pigments in textile applications are shown in **Table 3**. Dry rubbing fastness tends to be lower because mechanical action more easily disrupts the pigment–binder film at the fabric surface. The lower dry rubbing fastness in the 4M sample is likely due to higher pigment concentration reducing binder encapsulation, leaving more pigment exposed to surface abrasion.

**Table 3.** Rubbing Fastness Values

Variation	Condition	Rubbing fastness
<b>H1M</b>	Wet	4
	Dry	3-4
<b>H4M</b>	Wet	3-4
	Dry	2-3

The higher wet rubbing grades in this study contrast slightly with typical pigment behavior, where wet rubbing is usually weaker. This may be attributed to the crystalline and stable nature of hematite particles, which resist detachment even when moisture softens the binder layer (Opuchovic

& Kareiva, 2015). Similar behavior has been reported in studies where iron oxide pigments exhibit relatively stable wet rubbing resistance due to their density and low solubility (Fiuza et al., 2018).

Dry rubbing fastness showed slightly lower results due to the mechanical action weakening the binder film. Wet rubbing performed better, likely because hematite's particle stability prevents excessive pigment transfer. Unlike reactive or direct dyes, pigment coloration is limited to surface deposition rather than fiber penetration. This fundamental difference explains the dependence of pigment performance on binder adhesion rather than molecular affinity to the fiber. Consequently, properties such as rubbing fastness are more sensitive to surface film integrity compared to dye-based systems.

### 3.3 Washing Fastness

Both variations showed good washing fastness, with gray scale ratings of 3 for color change and 4–5 for staining as shown in **Table 4**. This is typical of pigment-based prints, since pigments do not chemically bind to cellulose fibers but are physically fixed via binder films. The washing performance indicates strong binder–pigment attachment and adequate film formation during curing.

**Table 4.** Gray and staining scale

Variation	H1M	H4M
<b>Gray scale for color change</b>	3	3
Rayon Acetate	4-5	4-5
Cotton	4-5	4-5
<b>Gray scale for staining</b>		
Nylon	4	4
Polyester	4-5	4-5
Acrylate	4-5	4-5
Wool	4-5	4-5

The excellent staining scale (4–5 across multifiber components) demonstrates that pigment migration during laundering is minimal. This matches findings from Galvão et al. (2018), who reported that hematite pigments exhibit high washing stability due to their insoluble and inert structure. During washing, mechanical agitation and interaction with detergent molecules can weaken the binder–fiber interface, potentially leading to pigment release. Nevertheless, the inherent insolubility and chemical stability of iron oxide pigments contribute to their relatively good washing fastness compared to many organic colorants (Galvão et al., 2018). These results indicate acceptable washing fastness due to effective binder-pigment fixation.

Despite the promising findings, this study has several limitations. Future work should focus on optimizing particle size, binder formulation, and curing conditions to enhance color strength and fastness properties. Additionally, advanced surface modification techniques may further improve pigment–binder interaction and overall performance in textile applications.

## 4. CONCLUSION

Hematite ( $\text{Fe}_2\text{O}_3$ ) derived from iron rust waste was successfully applied as a pigment in cotton textile printing, demonstrating good compatibility with conventional printing systems and reproducible coloration. The color strength increased slightly from  $1.13 \pm 0.09$  to  $1.22 \pm 0.10$  with increasing synthesis concentration, although the difference appears limited based on overlapping standard deviations. The printed fabrics exhibited consistent reddish-yellow hues with stable CIELAB values, indicating uniform pigment distribution. Washing fastness showed acceptable performance, with grade 3 for color change and 4–5 for staining, while rubbing fastness ranged from 2–4, reflecting moderate resistance to mechanical abrasion. These results confirm that rust-derived hematite is functionally applicable as a sustainable pigment for textile printing. However, the moderate color

strength and durability indicate that performance is strongly influenced by pigment–binder interaction and particle characteristics. Further optimization of particle size, dispersion, and binder formulation is necessary to enhance color depth and fastness for broader practical application.

## REFERENCES

- Bennett, P. (2019). Rust: An age old problem. *Materials Today*, 30, 103–104. <https://doi.org/10.1016/j.mattod.2019.09.019>
- Cahyana, A. H., Liandi, A. R., Reza, A. I., Wendari, T. P., & Hyun, P. K. (2024). Utilization of environmentally friendly catalyst Fe<sub>3</sub>O<sub>4</sub> from iron rust in the synthesis of spiropiperidine derivative. *Case Studies in Chemical and Environmental Engineering*, 9. <https://doi.org/10.1016/j.cscee.2023.100559>
- Chavan, V. D., Aziz, J., Kim, H., Patil, S. R., Ustad, R. E., Sheikh, Z. A., Patil, C. S., Chougale, M. Y., Sabale, S. R., Patil, S. A., Sutar, S. S., Kamat, R. K., Bae, J., Dongale, T. D., & Kim, D. kee. (2024). Transformation of rust iron into a sustainable product for applications in the electronic, energy, biomedical, and environment fields: Towards a multitasking approach. *Nano Today*, 54, 102085. <https://doi.org/10.1016/J.NANTOD.2023.102085>
- Choudhury, A. K. R. (2014). Object appearance and colour. In *Principles of Colour and Appearance Measurement* (pp. 53–102). Elsevier. <https://doi.org/10.1533/9780857099242.53>
- Choudhury, A. K. R. (2022). Principles of Textile Printing. In *Principles of Textile Printing* (pp. 55–114). CRC Press. <https://doi.org/10.1201/9781351067836-3>
- Cornell, R. M. ., & Schwertmann, Udo. (2003). *The iron oxides: structure, properties, reactions, occurrences, and uses*. Wiley-VCH.
- Fakhrudin, M. J. (2019). *Sintesis Pigmen Hematit ( $\alpha$ -Fe<sub>2</sub>O<sub>3</sub>) Dari Limbah Bubut Besi Dengan Variasi Waktu Sonikasi dan Aplikasinya Sebagai Anti Swelling Pada Kayu*.
- Fiuza, T. E. R., Borges, J. F. M., Cunha, J. B. M. da, Antunes, S. R. M., Andrade, A. V. C. de, Antunes, A. C., & Souza, É. C. F. de. (2018). Iron-based inorganic pigments from residue: Preparation and application in ceramic, polymer, and paint. *Dyes and Pigments*, 148, 319–328. <https://doi.org/10.1016/j.dyepig.2017.09.025>
- Galvão, J. L. B., Andrade, H. D., Brigolini, G. J., Peixoto, R. A. F., & Mendes, J. C. (2018). Reuse of iron ore tailings from tailings dams as pigment for sustainable paints. *Journal of Cleaner Production*, 200, 412–422. <https://doi.org/10.1016/j.jclepro.2018.07.313>
- Habibah, R. (2019). *Sintesis Pigmen Hematit ( $\alpha$ -Fe<sub>2</sub>O<sub>3</sub>) Dari Limbah Bubut Besi Dengan Variasi Konsentrasi Agen Pengendap Urea*.
- Katheresan, V., Kandedo, J., & Lau, S. Y. (2018). Efficiency of various recent wastewater dye removal methods: A review. In *Journal of Environmental Chemical Engineering* (Vol. 6, Number 4, pp. 4676–4697). Elsevier Ltd. <https://doi.org/10.1016/j.jece.2018.06.060>
- Khoiroh, L. M., Mardiana, D., Sabarudin, A., & Ismuyanto, B. (2013). Synthesis of Hematite Pigments ( $\alpha$ -Fe<sub>2</sub>O<sub>3</sub>) by Thermal Transformations of FeOOH. In *J. Pure App. Chem. Res* (Vol. 2, Number 1). [www.jpacr.ub.ac.id](http://www.jpacr.ub.ac.id)
- Legodi, M. A., & de Waal, D. (2007). The preparation of magnetite, goethite, hematite and maghemite of pigment quality from mill scale iron waste. *Dyes and Pigments*, 74(1), 161–168. <https://doi.org/10.1016/j.dyepig.2006.01.038>
- Li, X., Xi, F., Cheng, A., Zhou, P., Yang, B., Sun, H., Fu, G., Hou, R., Yang, R., Lu, W., Zhang, L., & Meng, X. (2025). Iron rust for efficient photocatalytic hydrogen evolution. *Journal of Colloid and Interface Science*, 695, 137849. <https://doi.org/10.1016/J.JCIS.2025.137849>

- Nurrahmajanti, A., & Lisdiana, A. (2025). Pengaruh Variasi Konsentrasi Asam dan Variasi Pengendap pada Sintesis Besi Oksida dari Limbah Karat Besi. *Insologi: Jurnal Sains Dan Teknologi*, 4(4), 822–830. <https://doi.org/10.55123/insologi.v4i4.6145>
- Opuhovic, O., & Kareiva, A. (2015). Historical hematite pigment: Synthesis by an aqueous sol–gel method, characterization and application for the colouration of ceramic glazes. *Ceramics International*, 41(3), 4504–4513. <https://doi.org/10.1016/J.CERAMINT.2014.11.145>
- Pfaff, G. (2020). Iron oxide pigments. *Physical Sciences Review*. [https://doi.org/10.1515/b\\_psr-2020-0179](https://doi.org/10.1515/b_psr-2020-0179)
- Yaseen, D. A., & Scholz, M. (2019). Textile dye wastewater characteristics and constituents of synthetic effluents: a critical review. In *International Journal of Environmental Science and Technology* (Vol. 16, Number 2, pp. 1193–1226). Center for Environmental and Energy Research and Studies. <https://doi.org/10.1007/s13762-018-2130-z>
- Yilidirim, F. F., Yavas, A., & Avinc Ozan. (2020). *Printing with Sustainable Natural Dyes and Pigments* (S. S. Muthu & M. A. Gardeti, Eds.; pp. 1–36). Springer. <http://www.springer.com/series/16490>